

Teleconnections between sea-surface temperature anomalies and air temperature in northeast Brazil

Vicente de P.R. Silva*, F.de A.S. Sousa, Enilson P. Cavalcanti,
Enio P. Souza, Bernardo B. da Silva

*Department of Atmospheric Sciences, Federal University of Campina Grande, Av. Aprígio Veloso, 882, Bodocongó,
Campina Grande 58 109-970, PB, Brazil*

Received 7 March 2005; received in revised form 13 December 2005; accepted 28 December 2005
Available online 21 February 2006

Abstract

The relationship between sea-surface temperature (SST) and air temperature in northeast Brazil was analyzed using sea-surface temperature anomalies (SSTA) and geographic coordinates. Mean monthly time series of air temperatures (daily mean, maximum and minimum) of 69 meteorological stations and SSTA from the Atlantic (North and South), the Global Tropics and the Pacific (Niño 3 area) Oceans were analyzed within the framework of principal component analysis (PCA) and linear regression approach. The PCA model was used to identify the dominant temporal and spatial variability patterns of air temperature estimated by the SSTA model and observed air temperature in northeast Brazil. The main objective of this research was to establish a predicting model from the geographic coordinates and SSTA, capable of reconstructing air temperature time series. Data analysis indicated statistically significant correlation ($p < 0.01$) between SST and air temperature. This relationship was less using the SST from the Equatorial Pacific Ocean (Niño 3 area) and it also proved to be statistically significant ($p < 0.01$). Results also showed that air temperature in northeast Brazil can be obtained with reasonable accuracy as a function of the geographic coordinates and SSTA. A substantial amount of data variance was accounted for by the first two components. The first and the second principal components (PC) of the mean daily air temperature time series, reconstructed on the basis of the SSTA, explained 90.2% (North Atlantic), 90.7% (South Atlantic), 91.5% (Global Tropics), 92.6% (Pacific Niño 3) and 64.4% (observed data) of the data variance. The first and the second PCs have been associated with the main atmospheric systems that act in northeast Brazil.

© 2006 Published by Elsevier Ltd.

Keywords: Principal component; El Niño/South Oscillation; SST anomalies; Atlantic Ocean; SSTA model

1. Introduction

The exchange of heat and mass between the Ocean and the atmosphere is strongly dependent on

the sea-surface temperature (SST) and it influences the weather and climate conditions on the continental areas. The supposed link between SST and air temperature over remote regions has led scientists to use the SST as an approach to obtain the air temperature in areas where these data are not available. The climate in northeast Brazil (hereafter NEB) is strongly influenced by sea-surface tempera-

*Corresponding author. Tel.: +55 83 3310 1202;
fax: +55 83 3310 1201.

E-mail address: vicente@dca.ufcg.edu.br (V.P.R. Silva).

ture anomalies (SSTA), mainly with the establishment of the dipole of the Atlantic Ocean (Moura and Shukla, 1981) and El Niño (Roucou et al., 1996). Other meteorological studies have focused teleconnection with SST in several parts of the world. Hong et al. (2001) established the relationship between the El Niño/South Oscillation (ENSO) and SST in the Sea of Japan; Lentini et al. (2001) investigated spatial and temporal SST variability in the Western region of the South Atlantic Ocean, and Konda et al. (2002) associated SST with seasonal changes in the monsoon circulation in the Indian Ocean.

Rainfall in tropical regions is very variable in time, space, duration and quantity whereas air temperature presents low variability. Therefore, it seems possible that air temperature can be easily simulated as a function of the geographic coordinates. In the absence of observed data, polynomial equation fit has been commonly used to obtain the air temperature by the least squares method. However, these prediction equations give only the mean air temperature as a function of geographic coordinates, which are not useful to predict air temperature time series for the locations without observed data (e.g., Russo et al., 1993; Cavalcanti and Silva, 1994; Bolstad et al., 1998).

Due to its great extension and location, NEB is influenced by several atmospheric systems, including the intertropical convergence zone, eastern waves, cold fronts and breezes and cyclonic upper air vortices (Roucou et al., 1996). The climate in NEB is characterized by low rainfall levels, high air temperatures and high evaporation rates. In this region, the high evaporative demand produces evaporation rates that can surpass 10 mm per day, whereas the mean air temperature varies between 12.8 and 40.1 °C.

Several researchers have analyzed the effect of the El Niño/Southern Oscillation (ENSO) phenomenon on surface air temperature and global and hemispheric temperatures (e.g., Jones, 1988; Privalsky and Jensen, 1995). More recently, researches have been conducted using principal component analysis (PCA) to study the SST variability. The PCA model indicates the dominant temporal and spatial variability patterns of the variables and links the particular modes to the physical processes (e.g., Park and Oh, 2000; Tseng et al., 2000; Hong et al., 2001; Rautenbach and Smith, 2001; Wilson-Diaz et al., 2001; Nielsen et al., 2002; Vargas et al., 2003). According to Preisendorfer (1988) the analysis of meteorological and oceanographic data is often

performed by means of PCA and its main objectives are to reduce the data, identify recurrent and independent characteristics and variation modes. The first PC mode explains most of the data variance; the second PC mode explains the next highest amount of the variance, and so on (Wilson-Diaz et al., 2001). Park and Oh (2000) investigated the interannual and interdecadal variability of the SST in the East Asian Marginal Seas using PCA and found that it was connected to the western equatorial Pacific. Vargas et al. (2003) used PCA to analyze the SST patterns in the Gulf of Cadiz. They observed that the first PC was correlated to the gradual warming of the study area, whereas the second mode is mainly responsible for the cooling the shelf waters in southwestern Iberia.

Air temperature data are scarcer and more difficult to obtain than those of sea water temperature. Therefore, the scientists who monitored the Earth's climate have used SST instead of air temperature, assuming that the two temperatures increase and decrease proportionally. Knowledge of air temperature is fundamental in several research areas, especially in meteorology, oceanography, climatology and hydrology. Nevertheless many air temperature prediction models give the monthly climatic mean alone. Hence they do not express the air temperature variation through time.

The objectives of the present paper are to investigate the link between SST and air temperature in NEB, to establish an air temperature prediction model as a function of the SSTA and the geographic coordinates and also to identify the dominant temporal and spatial variability patterns of air temperature in this region.

2. Data and methods

2.1. Study area

The analyses were carried out using both the linear regression approach and the PCA model to study the relationship between the SST and air temperature in NEB. The *t*-test was used to assess the statistical significance of the correlation coefficients between the observed air temperature and the simulated values as a function of the SSTA. The data used in this study consisted of monthly means of 69 air temperature time series (daily mean, maximum and minimum) of NEB (Table 1) and the SSTA from the North Atlantic (5–20°N, 60–30°W), the South Atlantic (0–20°S, 30°W–10°E), the Global

Table 1
Geographic coordinates of the meteorological stations used in the study

No.	Stations	Lat.	Long.	Elev.	No.	Stations	Lat.	Long.	Elev.
1	Turiacu	01°43'	45°24'	44	36	Recife	08°02'	34°53'	4
2	São Luiz	02°32'	44°18'	50	37	Paulistana	08°20'	41°09'	350
3	Parnaíba	02°55'	41°47'	15	38	Arcoverde	08°26'	37°04'	663
4	Sobral	03°42'	40°21'	75	39	Pesqueira	08°22'	36°42'	650
5	Zé Doca	03°43'	45°32'	528	40	Cabrobó	08°30'	39°19'	350
6	Fortaleza	03°44'	38°32'	26	41	Floresta	08°36'	38°35'	317
7	Carolina	07°20'	47°28'	192	42	Garanhuns	08°52'	36°29'	866
8	Caxias	04°52'	43°21'	103	43	Alto Parnaíba	09°07'	45°57'	285
9	Teresina	05°04'	42°49'	72	44	P. de Pedras	09°10'	35°18'	22
10	Morada Nova	05°06'	38°23'	50	45	Caracol	09°17'	43°19'	556
11	Macau	05°07'	36°38'	2	46	Água Branca	09°17'	37°56'	510
12	Cratueus	05°11'	40°40'	275	47	Paulo Afonso	09°21'	38°15'	250
13	Quixeramobim	05°12'	39°18'	187	48	Petrolina	09°23'	40°30'	376
14	Mossoró	05°12'	37°21'	15	49	P. dos Índios	09°24'	36°39'	342
15	Barra do Corda	05°30'	45°16'	153	50	Remanso	09°41'	42°04'	378
16	Imperatriz	05°32'	47°30'	123	51	Coruripe	10°07'	36°10'	10
17	Apodi	05°40'	37°48'	305	52	Propriá	10°13'	36°50'	17
18	Natal	05°48'	35°13'	8	53	S. do Bonfim	10°27'	40°11'	544
19	Tauá	06°01'	40°26'	356	54	Aracaju	10°54'	37°03'	3
20	Colinas	06°03'	44°15'	179	55	Barra	11°5'	43°09'	410
21	Florânia	06°07'	36°49'	210	56	Jacobina	11°10'	40°31'	460
22	Iguatu	06°22'	39°18'	213	57	Itabaianinha	11°16'	37°47'	225
23	Cruzeta	06°25'	36°47'	140	58	Irecê	11°18'	41°52'	722
24	Florianópolis	06°46'	43°01'	85	59	M. do Chapéu	11°32'	41°08'	1012
25	São Gonçalo	05°20'	38°44'	120	60	Alagoinhas	12°08'	38°25'	140
26	Patos	07°01'	37°17'	250	61	Itaberaba	12°32'	40°18'	270
27	Campos Sales	07°04'	40°23'	551	62	Lençóis	12°34'	41°23'	394
28	Picos	07°04'	41°28'	195	63	Salvador	13°01'	38°31'	10
29	João Pessoa	07°07'	34°53'	5	64	B. J. da Lapa	13°16'	43°25'	435
30	C. Grande	07°13'	35°52'	508	65	Itirucu	13°32'	40°08'	820
31	Barbalha	07°19'	39°19'	405	66	Caetite	14°04'	42°29'	826
32	Balsas	07°53'	46°03'	259	67	Carinhanha	14°18'	43°46'	452
33	Triunfo	07°50'	38°07'	1010	68	Ilheus	14°48'	39°18'	45
34	Surubim	07°50'	35°45'	380	69	Canavieiras	15°40'	38°57'	4
35	Monteiro	07°53'	37°07'	590					

Tropics (10°S–10°N, 0–360°) and the Tropical Pacific Oceans (Niño 3 area)(5°N–5°S; 150–90°W).

Fig. 1 shows the location of NEB and the meteorological stations used in this study. The SSTA time series (as given by NOAA, 2003) and air temperature cover a time span of 30 years, from 1961 to 1990. NEB occupies an area of approximately 1.5 million square kilometers and it is located between 48°05'W–35°02'W and 1°02'S–8°05'. This extensive region is bathed on the North and East by the Atlantic Ocean.

2.2. Air temperature estimative model

The air temperature time series of 69 meteorological stations spread over the study region were

reconstructed as a function of their geographic coordinates (i.e., latitude, longitude and elevation) and the SSTA. The empirical model of air temperature estimation is a quadratic surface, given as follows:

$$T_{ij} = a_0 + a_1\lambda + a_2\phi + a_3h + a_4\lambda^2 + a_5\phi^2 + a_6h^2 + a_7\lambda\phi + a_8\lambda h + a_9\phi h + SSTA_{ij}, \quad (1)$$

where a_0, \dots, a_9 are the regression coefficients, λ is longitude, ϕ is latitude and h elevation of each meteorological station analyzed. The indices i and j indicate, respectively, the month and year to which the air temperature (T_{ij}) is estimated. Thus, the $SSTA_{ij}$ sign assumes positive and negative values according to the SST patterns modeled over the analyzed Oceans.

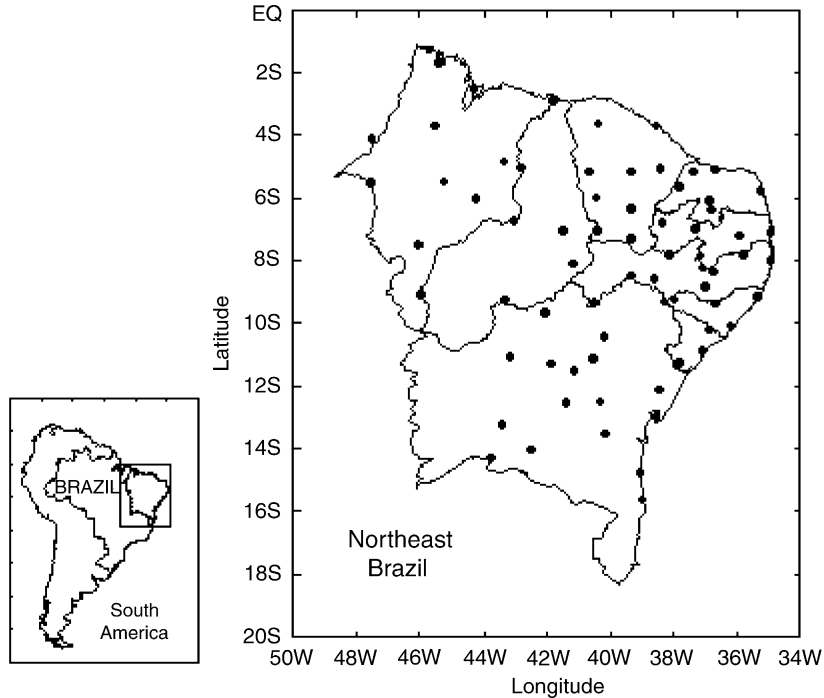


Fig. 1. Map of South America including northeast Brazil (study area) with delimitation of the nine states of the region. The black dots correspond to the meteorological stations used in the research.

2.3. Principal component analysis

In this research the PCA model was applied to the observed and simulated air temperature time series to identify the spatial variation pattern of this climatic variable in NEB. The PCA model was run on the correlation matrix so that the spatial oscillations could be shown. From the original data matrix (with $n \times m$ dimension), a square and symmetrical correlation (R_n) matrix was extracted. In the sequence using R_n and the identity matrix (I_n), n eigenvalues (λ_n) were derived as follows:

$$\det[{}_n R_n - \lambda_n I_n] = 0. \quad (2)$$

For each eigenvalue (λ_n) of the equation above (i.e., characteristic equation) a vector different from zero (e_1) was obtained by equation

$${}_n R_n e_1 = \lambda_n e_1, \quad (3)$$

where e_1 is the eigenvector of the R_n correlation matrix associated to its corresponding eigenvalue. The eigenvectors derived from the correlation matrix represent the mutual orthogonal linear combinations of this matrix. The associated eigenvalues quantify the total variance explained by each

one of the eigenvectors. Most of the total data variance can be explained when only the first pairs of eigenvector/eigenvalue or principal components are retained. The higher-order main components, which explain a minimum quantity of the total data variance (i.e., noise) can be ignored. The Scree Test method was used to establish the number of principal components to be retained. The fraction of the total variance explained by the first components retained is then obtained by the percentage of the explained variance (PEV) as follows:

$$\text{PEV} = \left(\frac{\sum_i \lambda_i}{\sum_n \lambda_n} \right) 100 (\%). \quad (4)$$

The air temperature data that originally contained n interrelated variables were reduced to contain only the first significant variables, which are orthogonal and consequently independent (main components). Furthermore, this procedure explains most of the total data variance. The elements of each eigenvector were multiplied by the square root of the associated eigenvalue to obtain the weights of the components. These weights represent the correlation between the principal components and the n variables (meteorological station distributed

spatially in the study region). Alternatively, the weights determine the similarity (interrelated among the n variables) between the variables and the principal components. The weight sum of squares (L^2) indicates the total variance explained by the component (eigenvalue) and is given as

$$\lambda_i = \sum_j L_{ij}^2. \quad (5)$$

Although the objective of the PCA model is to identify spatial variation and to delimit sub-regions (by similarity of the variables), it is advisable to rotate the initial solution to a new vector coordinate to highlight the interpretation of the system. The oblique and orthogonal rotations are the main types of axe rotations available in PCA. The Varimax orthogonal method was used in this research because it rotates rigidly the required principal components. Therefore, this procedure provides a clearer way for identifying the different groups that contain interrelated variables, as well as keeping the individual restriction of each principal component.

3. Results and discussion

Figs. 2–4 show the spatial distribution of the correlation coefficients between observed air temperature (daily mean, minimum and maximum) in NEB and simulated values on the basis of SSTA. Shaded areas represent correlation coefficients superior to 0.8 and all of them were statistically significant ($p < 0.01$). The maps of correlation coefficients are shown in Fig. 2d (daily mean air temperature), Fig. 3d (minimum air temperature) and Fig. 4d (maximum air temperature). Privalsky and Jensen (1995) showed a linear relationship between the South Oscillation index and global air temperature, which was statistically significant at the 90% confidence level. Cavalcanti and Silva (1994) adjusted a quadratic surface as a function of the geographic coordinates to estimate the monthly mean air temperature in NEB and thus obtained correlation coefficients ranging from 0.76 to 0.99.

The shaded area ($r > 0.8$) is greater when the mean daily air temperature time series were reconstructed as a function of the SSTA from the North Atlantic (Fig. 2a), the South Atlantic (Fig. 2b) and the Global Tropics Oceans (Fig. 2c). The relationship between the mean daily air temperature predicted on the basis of the SSTA from the Pacific Ocean (El Niño 3 area) and the observed data showed

correlation coefficient less than 0.8 in practically all the study area (Fig. 2d). When the relationship is based on observed minimum and maximum air temperatures in NEB and SSTA from these Oceans, the correlation coefficients are also relatively low (see Figs. 3d and 4d) but they are statistically significant ($p < 0.01$). These results confirm the hypothesis that the SST of the Pacific Ocean (El Niño 3 area) has less influence on the air temperature in NEB than the SST of the North Atlantic, South Atlantic and Global Tropics Oceans. Hence it seems evident that the air temperature advection in the Ocean–Earth system (i.e. heating or cooling on the continent) is strongly affected by the distance between the correlated areas.

The maps of the spatial distribution of the correlation coefficients between the observed minimum air temperature time series and time series simulated by the SSTA from the North Atlantic (Fig. 3a), the South Atlantic (Fig. 3b) and the Global tropical Oceans (Fig. 3c) showed $r > 0.8$ at the East Coast and greater part of the South region of NEB. The relationships with the air temperature time series predicted by the SSTA model with data from the Pacific Ocean (El Niño 3 area) are small, despite only few nuclei of $r > 0.8$ located at the South and Southeast and another very small nucleus at the Center of the study region (Fig. 3d). The minimum air temperature in NEB is better correlated with the SST of the Global Tropics (see shaded area with $r > 0.8$) than with SST of the Pacific Ocean (El Niño 3 area).

Fig. 4 shows the spatial distribution of the correlation coefficients between observed maximum air temperature in NEB and those simulated on the basis of SSTA from the Atlantic (North and South), the Pacific and the Global Tropic Oceans. The relationship between variables is greater with the SST of the North Atlantic and the Global Tropics Oceans than with SST of the South Atlantic and the Pacific Oceans. The correlations maps of the air temperature obtained on the basis of SSTA from the North Atlantic SSTA (Fig. 4a) and Global Tropics (Fig. 4c) showed two areas with $r < 0.8$, which are located at the Center-East and the North Coast of the study region. Many correlation coefficients between the observed air temperature time series (daily mean, minimum and maximum) and simulated time series based on SSTA from the Pacific Ocean (El Niño 3) were also less than 0.8. Despite the existence of correlation coefficient nucleus of 0.6, located in southwest of the study region, all the

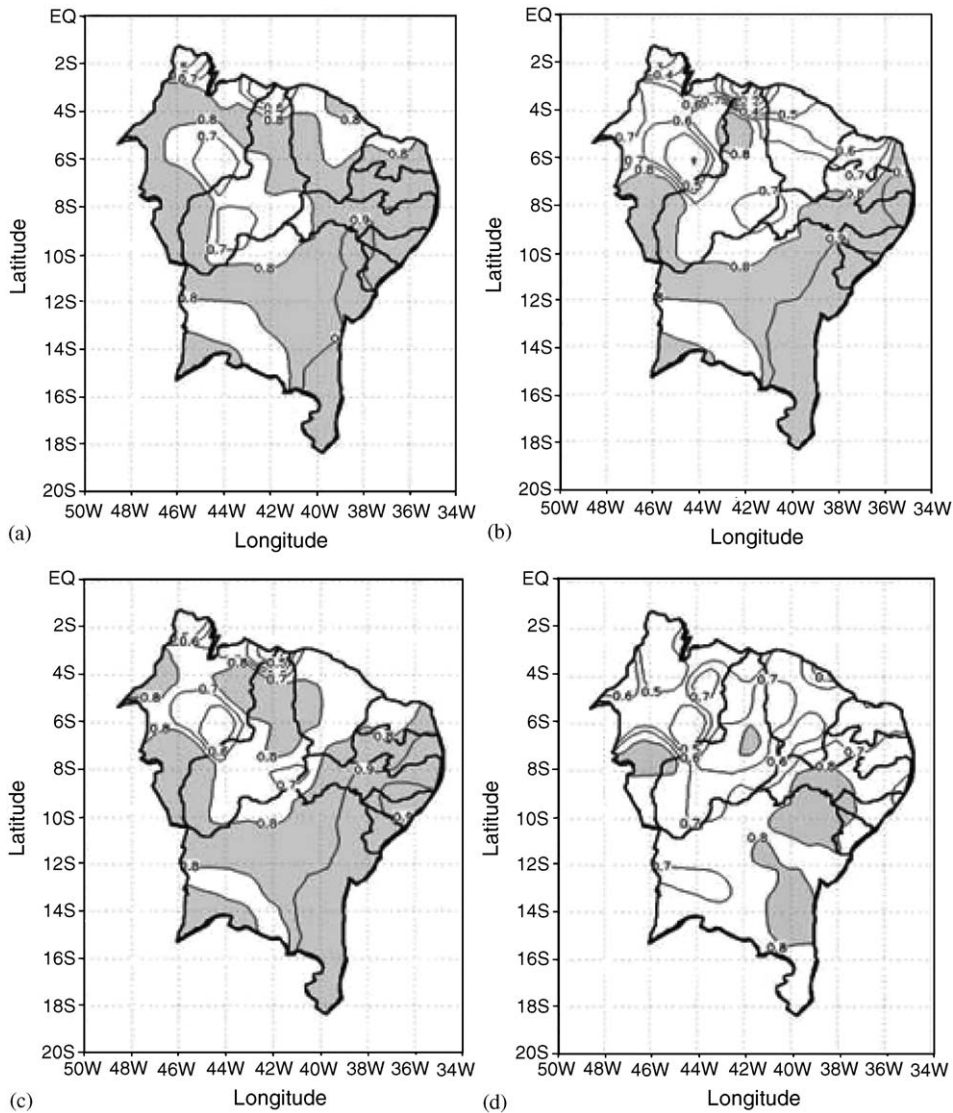


Fig. 2. Spatial distribution of the correlation coefficients between the observed mean daily air temperature in northeast Brazil and the values simulated on the basis of the SSTA model for the Oceans: (a) the North Atlantic, (b) the South Atlantic, (c) the Global Tropics and (d) the Pacific (El Niño 3 area).

relationships between time series were statistically significant ($p < 0.01$) according to the t -test. The highest correlation coefficient (shaded area) is located in the East and North of NEB (Fig. 4d).

For all the analyzed Oceans, the observed air temperature (mean daily, minimum and maximum) over the East coast (i.e., between latitudes 40°W–35°W) were well correlated to the air temperature simulated by SSTA model. On the other hand, the North coast of the study region showed correlation coefficients less than 0.8 between observed air temperature (mean daily and

minimum air temperature) and estimated values based on the SSTA from the North Atlantic and the Global Tropics Oceans. This same area of NEB showed correlations greater than 0.8 when the association was made with maximum air temperature. The variability of the correlation coefficients is due to influence of many processes responsible in large part by atmospheric dynamical instability. Other researchers have assessed the influence of physical phenomena on air temperature. For example, Butler and Johnson (1996) confirmed the link between solar activity and mean air tempera-

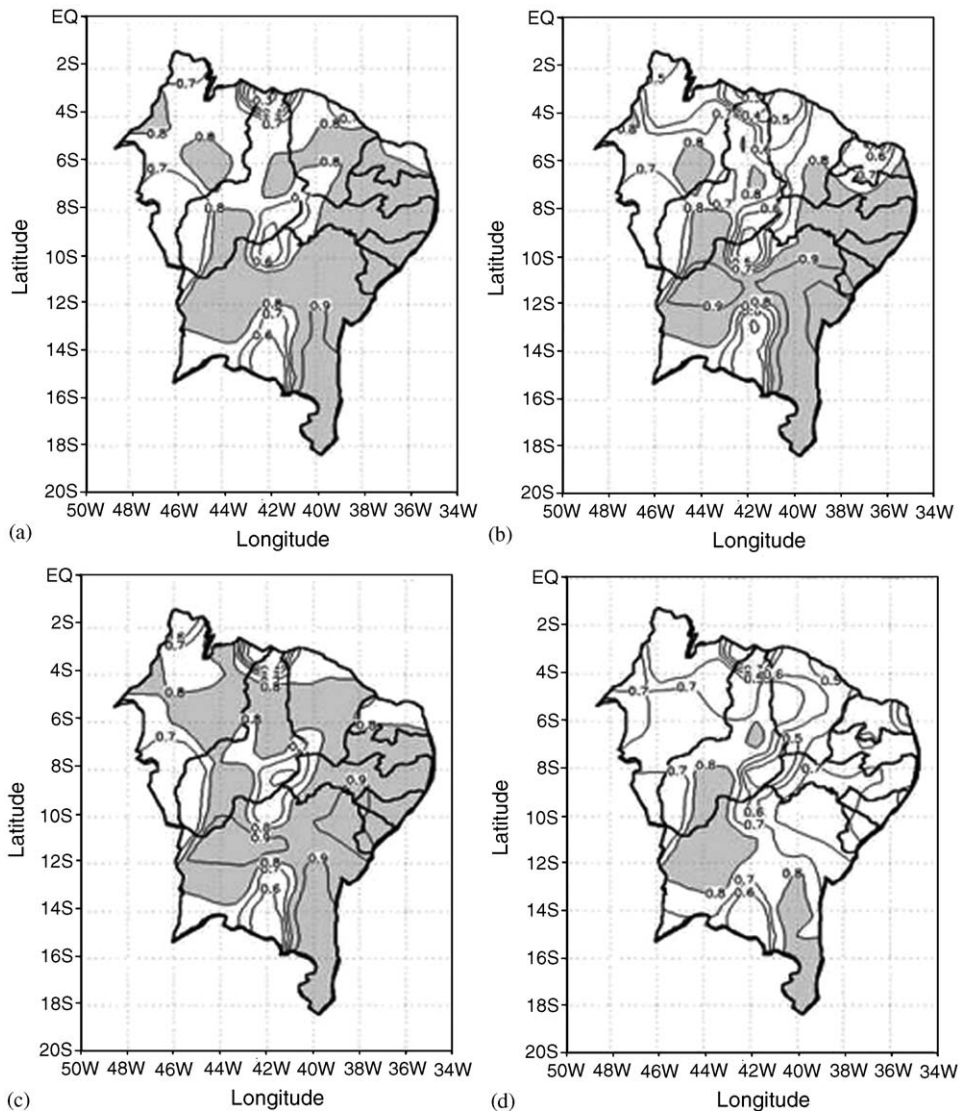


Fig. 3. Spatial distribution of the correlation coefficients between the observed minimum air temperature in northeast Brazil and the values simulated on the basis of the SSTA model for the Oceans: (a) the North Atlantic, (b) the South Atlantic, (c) the Global Tropics and (d) the Pacific (El Niño 3 area).

ture; Privalsky and Jensen (1995) assessed the influence of the ENSO phenomenon on global air temperature. Vadász (1994) studied the relationship between air temperature and the vegetation index and Wilson (1999) analyzed the correlation between air temperature and El Niño 3 area and volcanic eruptions.

Fig. 5 shows the temporal behavior of the observed mean daily air temperatures in Campina Grande station ($07^{\circ}13'S-35^{\circ}W$) and estimated by the SSTA model from 1961 to 1990. The analysis of these figures suggests the existence of a lag of some months between the observed air temperature and

values estimated by the SSTA model due to the delay of the atmosphere over the continent in response to the SST variations. The influence of this lag on the estimated air temperature was not investigated in the present study. The observed mean air temperature time series has also been fitted well to the simulated air temperature time series based on SSTA from the North Atlantic (Fig. 5a), the South Atlantic (Fig. 5b) and the Global Tropics Oceans (Fig. 5c). The relationship between the time series showed correlation coefficients greater than 0.9 except when it was associated with anomalies data from Pacific Ocean. The air temperature

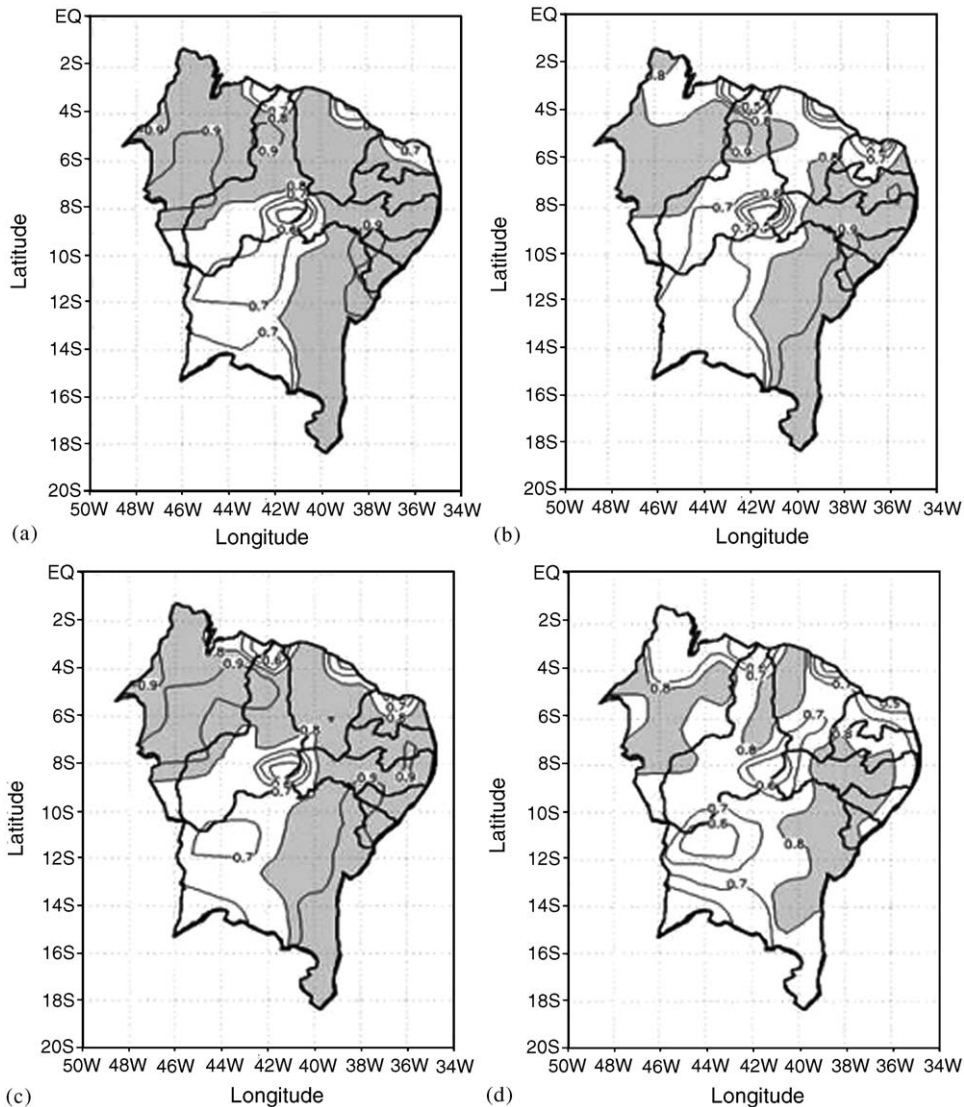


Fig. 4. Spatial distribution of the correlation coefficients between the observed maximum air temperature in northeast Brazil and the values simulated on the basis of the SSTA model for the Oceans: (a) the North Atlantic, (b) the South Atlantic, (c) the Global Tropics and (d) the Pacific (El Niño 3 area).

annual cycle showed an increase trend, which was perfectly reproduced by SSTA model. However, the air temperature data based on the SSTA model with data from the Pacific Ocean (El Niño 3 area) had less fitting (Fig. 5d), with a correlation coefficient of 0.76. The simulated data showed a tendency to overestimate the observed mean daily air temperature data during the period analyzed. These results suggest that the air temperature (daily mean, maximum and minimum) in NEB could be predicted with reasonable level of accuracy as a function of the SSTA from the North Atlantic, the South Atlantic and the Global Tropics Oceans. Sun

and Furbish (1997) also observed that the annual rainfall and steam discharge quantity over the Florida Peninsula could be predicted from the SST anomalies from the Eastern Tropical Pacific. Roy and Reason (2001) using a simple linear correlation model reported a correlation coefficient of 0.73 between the ENSO and SST anomalies.

From the PCA application, results suggest the retention of the first two principal components (i.e., CP₁ and CP₂) and the truncation (considered as noise) of the higher-order principal components (i.e., CP₃, CP₄, ... CP₆₉). The summary of this application is synthesized in Table 2, which shows

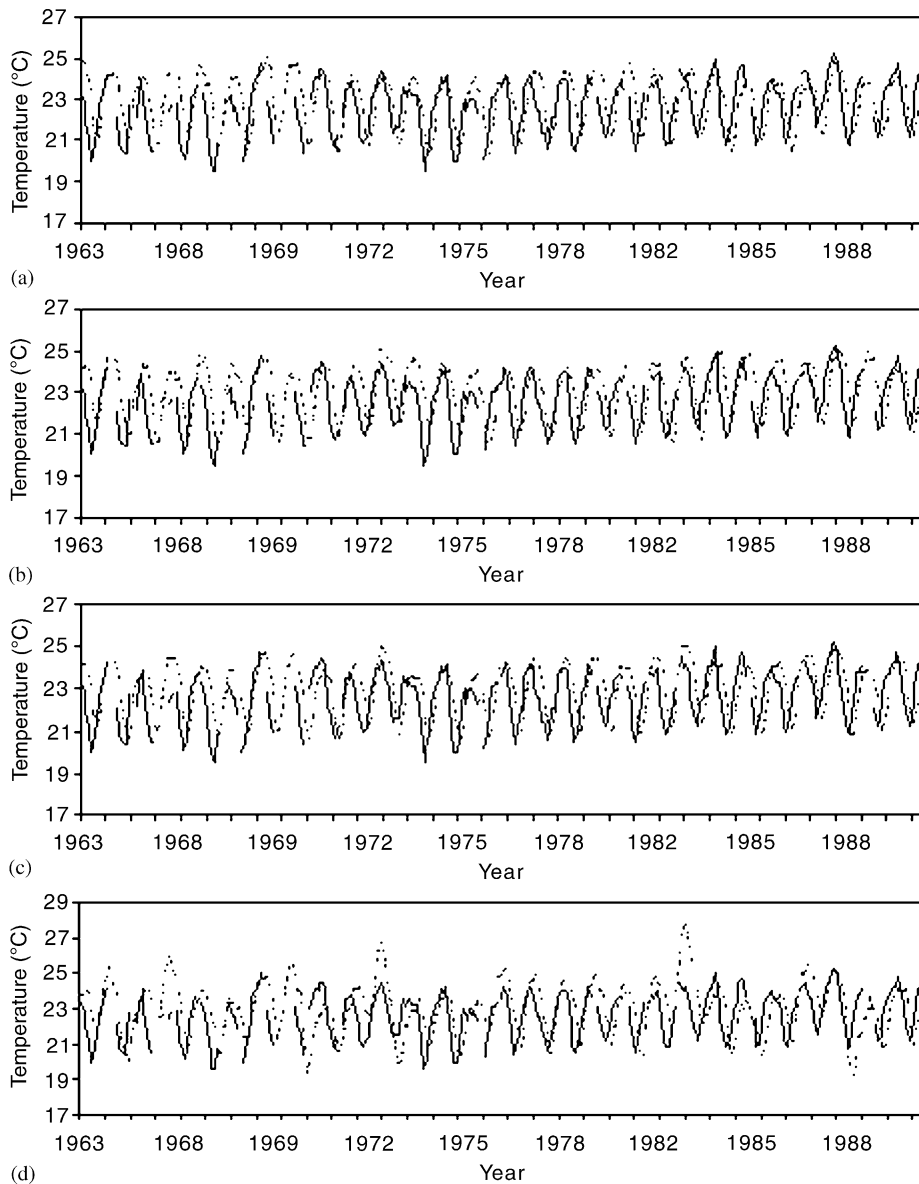


Fig. 5. Comparison between the observed mean daily air temperature (solid line) in Campina Grande ($07^{\circ}13'S-35^{\circ}52'W$) and the values simulated (dotted line) based on the SSTA model for the Oceans: (a) the North Atlantic ($r = 0.92$); (b) the South Atlantic ($r = 0.94$); (c) the Global Tropics ($r = 0.94$) and (d) the Pacific (El Niño 3 area) ($r = 0.76$).

the sum of squares loading, explained variance, cumulated explained variance and cumulated sum of squares loading of the first two principal components. The total variance explained by the first principal component (CP_1) of the mean daily air temperature obtained by the SSTA model from the North Atlantic (54.6%), the South Atlantic (57.3%) the Global Tropics (56.6%) and the Pacific Oceans (El Niño 3 area) (56.2%) was greater than the explained variance of the observed air tempera-

ture in NEB (33.9%). This same behavior also occurred with the variance explained by the second principal component (CP_2) and obviously, with cumulated explained variance of the two components (i.e., the North Atlantic: 90.2%; the South Atlantic: 90.7%; the Global Tropics: 91.5% and the Pacific (El Niño 3 area): 92.6%). The cumulated explained variance of the observed air temperature in NEB was 64.4%. This low value is attributed to possible gaps in the time series, which did not harm

Table 2

Statistics of the two rotated principal components of the estimated air temperatures on the basis of the SSTA from: the North Atlantic, the South Atlantic, the Global Tropics and the Pacific (El Niño 3 area) Oceans

	Components\Temperatures	North Atlantic	South Atlantic	Global tropics	Pacific Niño 3	Observed
PC ₁	Sum of squares loadings	37.6	39.5	39.1	38.8	22.1
	Explained variance (%)	54.6	57.3	56.6	56.2	33.9
PC ₂	Sum of squares loadings	24.6	23.1	24.1	25.1	19.8
	Explained variance (%)	35.7	33.5	34.9	36.4	30.5
PC ₁ +PC ₂	Cumulated loadings	62.2	62.6	63.2	63.9	41.9
	Cumulated variance (%)	90.2	90.7	91.5	92.6	64.4

the analysis. The missing air temperature data were replaced by climatological mean value.

According to the results, the first PC represents the seasonal heating and cooling of the atmospheric air caused by the influence of the dynamic systems that act on the East coast of NEB (e.g., frontal systems, easterly breezes and cyclonic vortexes). The second mode has been associated to the seasonal migration of the intertropical convergence zone that acts on the north coast of NEB. Mavor and Bisagni (2001) studied the seasonal variability of the SST on Georges Bank. They showed that the spatial patterns of the first PC mode was most linked to the Scotian Shelf Water flows across the Northeast Channel, while the second mode indicated the development of the “hot spot” often observed over Georges Bank during the late summer and early fall.

Fig. 6 plots the principal components spatial pattern of the mean daily air temperature in NEB. The meteorological stations located in the shaded area form group 1 or CP₁, while the meteorological stations located in the clear area form group 2 or CP₂. Except for the meteorological stations of Colinas (06°03'S–44°15'W) and Balsas (07°53'S–46°03'W), located in the unshared area of the Figs. 6b–d, the mean daily air temperatures estimated by the SSTA model showed an excellent pattern of spatial distribution. This also occurred when the estimated air temperature values were compared with the observed values. In other words, the spatial pattern of air temperature based on the SSTA model agrees well with the spatial pattern of observed air temperature in the study region.

The PCA model also revealed a strong correlation between SST and air temperature over NEB. Observed and estimated air temperature time series presented a pattern behavior relatively homogeneous and also a similar spatial variability. Results from the PCA model also showed that the simulated air temperature on the basis of SSTA from the

North Atlantic, the South Atlantic, the Global Tropics and the Pacific Oceans (El Niño 3 area) agree very well with the observed air temperatures in NEB. Rautenbach and Smith (2001) also used the PCA model and found teleconnections between SST and the rainfall over southern Africa.

4. Summary and conclusions

This study investigated the influence of SST of the North Atlantic, the South Atlantic, the Global Tropics and the Pacific Oceans (El Niño 3 area) on the air temperatures in northeast Brazil. The paper emphasizes that the statistically significant correlation coefficients ($p < 0.01$) characterize the connection between SST and air temperature in NEB. Although the relationship between observed and simulated air temperature has been less with SSTA from the Equatorial Pacific Ocean (El Niño 3 area), all the correlation coefficients were statistically significant ($p < 0.01$).

The prediction model (SSTA model) presented in this study can be used with reasonable level of accuracy to reconstruct air temperature time series in NEB. The SSTA from the North Atlantic, the South Atlantic and the Global Tropics Oceans were better predictors of air temperature in NEB than the SSTA from the Pacific Ocean (El Niño 3 area). The air temperature (daily mean, maximum and minimum) of the east coast of NEB, which includes an extensive area between the longitudes 40°W–35°W, is strongly influenced by the SST of the North Atlantic, the South Atlantic and the Global Tropics Oceans. The area located in central west of NEB presented $r < 0.8$ between observed maximum air temperature and values simulated by the SSTA model for all the Oceans.

The observed daily mean air temperature time series showed a similar temporal behavior to the values simulated by the SSTA model for the

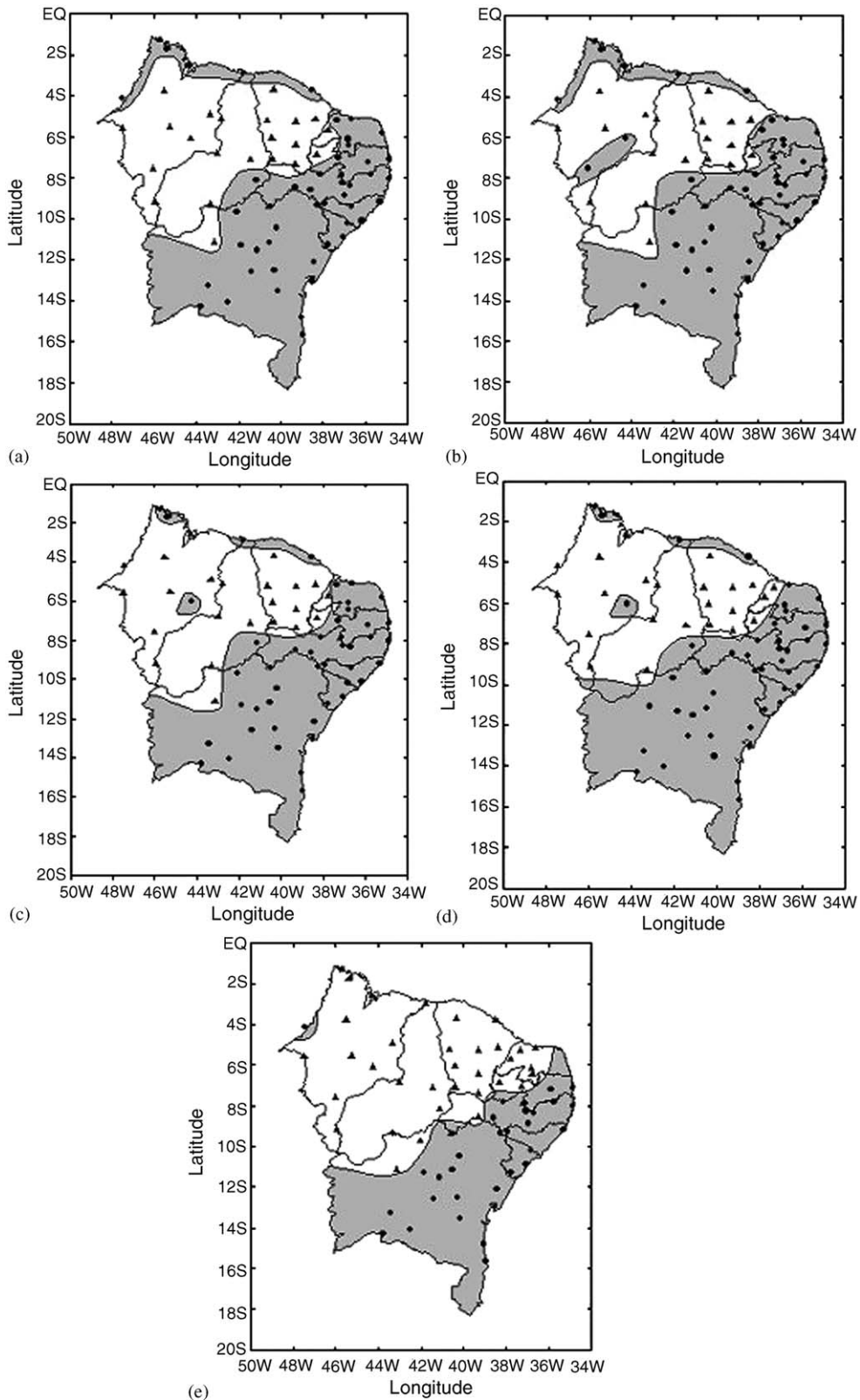


Fig. 6. Principal components spatial patterns of air temperature over NEB estimated on the basis of the SSTa from Oceans: (a) the North Atlantic, (b) the South Atlantic, (c) the Global Tropics and (d) the Pacific (El Niño 3 area) and (e) observed data.

location of Campina Grande. The correlation coefficient between them was greater than 0.9 except for the estimated air temperatures based on the SSTa from the Pacific Ocean (El Niño 3 area), which was 0.76. In this station the air temperatures ranged from 14.5 in winter to 33.2 °C in summer with a mean value of 23 °C. The seasonal cycle (winter–summer) is perfectly reproduced by SSTa model. The temporal behavior of the two air temperatures time series showed a slight tendency to increasing during the period analyzed (1961–1990). The PCA model showed that a substantial amount of variance in the air temperature data was accounted for by the first two components, which are associated to the main atmospheric systems that act in northeast Brazil, such as frontal systems, easterly breezes, cyclonic vortexes of the intertropical convergence zone.

References

- Bolstad, P.V., Swift, L., Collins, F., Régnière, J., 1998. Measured and predicted air temperature at basin to regional scales in the southern Appalachian mountains. *Agricultural and Forest Meteorology* 91, 161–176.
- Butler, C.J., Johnston, D.J., 1996. A provisional long mean air temperature series for Armagh Observatory. *Journal of Atmospheric and Terrestrial Physics* 58, 1657–1672.
- Cavalcanti, E.P., Silva, E.D.V., 1994. Estimativa da temperatura do ar em função das coordenadas locais. In: XII Congresso Brasileiro de Meteorologia e II Congresso Latino-Americano de Ibérico de Meteorologia, vol. 1. Sociedade Brasileira de Meteorologia, Anais, pp. 154–157.
- Hong, C.-H., Cho, K.-D., Kim, H.-J., 2001. The relationship between ENSO events and sea surface temperature in the East (Japan) Sea. *Progress in Oceanography* 49, 21–40.
- Jones, P.D., 1988. The influence of ENSO on global temperatures. *Climate Monitor* 17, 81–89.
- Konda, M., Imasato, N., Shibata, A., 2002. Interannual variability of the sea-surface temperature in the Indian Ocean in response to the air–sea turbulent heat exchange. *Deep-Sea Research II* 49, 1527–1548.
- Lentini, C.A.D., Podestá, G.G., Campos, E.J.D., Olson, D.B., 2001. Sea surface temperature anomalies on the Western South Atlantic from 1982 to 1994. *Continental Shelf Research* 21, 89–112.
- Mavor, T.P., Bisagni, J.J., 2001. Seasonal variability of sea-surface temperature fronts on Georges Bank. *Deep-Sea Research II* 48, 215–243.
- Moura, A.D., Shukla, J., 1981. On the dynamics of droughts in North-East Brazil: observations, theory and numerical experiments with a general circulation model. *Journal Atmospheric Science* 38, 2653–2675.
- Nielsen, A.A., Conradsen, K., Andersen, O.B., 2002. A change oriented extension of EOF analysis applied to the 1996–1997 AVHRR sea surface temperature data. *Physics and Chemistry of the Earth* 27, 1379–1386.
- NOAA, 2003. Climate Prediction Center/Monthly Atmospheric Indices. <http://www.cpc.noaa.gov/data/indices/index.html>
- Park, W.S., Oh, I.S., 2000. Interannual and interdecadal variations of sea surface temperature in the East Asian Marginal Seas. *Progress in Oceanography* 47, 191–204.
- Preisendorfer, R.W., 1988. Principal component analysis in meteorology and oceanography. In: Mobley, C.D. (Ed.), *Developments in Atmospheric Science*, p. 17.
- Privalsky, V.E., Jensen, D.T., 1995. Assessment of the influence of ENSO on annual global temperature. *Dynamics of Atmospheres and Oceans* 22, 161–178.
- Rautenbach, C.J.deW., Smith, I.N., 2001. Teleconnections between global sea-surface temperature and the interannual variability of observed and model simulated rainfall over southern Africa. *Journal of Hydrology* 254, 1–15.
- Roucou, P., Aragão, J.O.R., Harzallah, A., Fontaine, B., Janicot, S., 1996. Vertical motion, changes to Northeast Brazil rainfall variability: a GCM simulation. *International Journal of Climatology* 16, 879–891.
- Roy, C., Reason, C., 2001. ENSO related modulation of coastal upwelling in the eastern Atlantic. *Progress in Oceanography* 49, 245–255.
- Russo, J.M., Liebhold, A.M., Kelley, J.G.W., 1993. Mesoscale weather data response as input to a gypsy moth (*Lepidoptera: Lymantriidae*) phenology model. *Journal of Economic Entomology* 86, 838–844.
- Sun, H., Furbish, D.J., 1997. Annual precipitation and river discharges in Florida in response to El Niño-and La Niña-sea surface temperature anomalies. *Journal of Hydrology* 199, 74–87.
- Tseng, C., Lin, C., Chen, S., Shyu, C., 2000. Temporal and spatial variations of sea surface temperature in the East China Sea. *Continental Shelf Research* 20, 373–387.
- Vadász, V., 1994. On the relationship between surface temperature, air temperature and vegetation index. *Advanced Space Research* 14, 41–44.
- Vargas, J.M., Garcia-Lafuente, J., Delgado, J., Criado, F., 2003. Seasonal and wind-induced variability of sea surface temperature patterns in the Gulf of Cádiz. *Journal of Marine Systems* 38, 205–219.
- Wilson, R.M., 1999. Variation of surface air temperature in relation to El Niño and cataclysmic volcanic eruptions, 1796–1882. *Journal of Atmospheric and Solar-Terrestrial Physics* 61, 1307–1319.
- Wilson-Diaz, D., Mariano, A.J., Evans, R.H., Luther, M.E., 2001. A principal component analysis of sea-surface temperature in the Arabian Sea. *Deep-Sea Research II* 48, 1097–1114.